Measurement of the apex temperature of a nanoscale semiconducting field emitter illuminated by a femtosecond pulsed laser

A Kumar[1,2], J Bogdanowicz[1], J Demeulemeester[1], J Bran[1,2], D Melkonyan[1,2], C Fleischmann[1] and W Vandervorst[1,2]

Corresponding author: arul.kumar@imec.be

[1]Imec vzw, Kapeldreef 75, Heverlee – 3001, Belgium
[2] Instituut voor Kern- en Stralingsfysica, KU Leuven, Celestijnenlaan 200D, B-3001 Leuven, Belgium

Evaluating the thermal processes occurring inside an illuminated nanoscale semiconducting tip is of the utmost importance for the physical understanding of laser assisted atom probe tomography (L-APT). In this paper, we present a methodology to evaluate the temperature at the apex of the tip using L-APT. The method is based on the known exponential dependence of the probability for field evaporation on the temperature and the electric field at the apex. We use this method to gain insights into the effect of tip shape, doping and laser power on the peak temperature reached at the apex of an illuminated Si tip.

1. Introduction

The thermal effects induced by light interacting with a nanometer scale tip are of interest for many metrology techniques such as photo-assisted scanning tunneling microscopy (STM), laser-assisted atom probe tomography (L-APT), Atomic Force microscope-assisted surface modification and nanofabrication, apertureless near-field optical microscopy (a-SNOM) etc. On the one hand, techniques like STM and a-SNOM primarily use a pulsed laser to enhance the resolution, sensitivity or the scope of application using optical phenomena like nanoscopic scattering, second harmonic generation, single- or two-photon fluorescence [1–4]. However, the laser in these techniques also induces heating in the substrate and the tip, which might adversely affect the quality of the measurement. On the other hand, in techniques like L-APT, a pulsed laser is purposefully used to generate thermal pulses in the tip [4]. In L-APT, time-controlled atom-by-atom field evaporation is indeed achieved by the combined effects of a constant voltage and a laser pulse. The electric field induced at the tip apex by the applied voltage lowers the potential barrier for atom ionization and desorption, while the laser pulse induces a nanosecond thermal pulse which provides the necessary energy for the atom to cross the barrier. The relation between the laser characteristics (e.g. power, wavelength and pulse length) and the resulting temperature at the apex of the tip is key for a quantitative description of the

role of the laser pulse and its effect on spatial and mass resolution [5], quantification [6,7], surface migration [8] etc. However, modelling and understanding the interaction between the ultra-short laser pulse and the sub-wavelength tip remains a challenge as it involves concurrent processes of absorption, excited carrier generation, carrier migration and tip cooling on short time scales (picosecond-nanosecond)[4]. That being said, L-APT is also uniquely suited for studying the thermal effects induced by the laser inside a tip-shaped sample because the probability of emission of an atom in L-APT is a very sensitive – exponential-function of the temperature at the apex of the illuminated tip [9]. This implies that the rate at which atoms are field evaporated can act as a probe for the thermal response of the tip. Methods to quantify the temperature at the apex of a biased tip have been proposed using a combination of laser-assisted and pulsed-voltage APT [10,11]. Unfortunately, they rely on the propagation of high-voltage pulses through the tip, which is nearly impossible for semiconductors and insulators without excessive dispersion [12], thereby, limiting the accuracy of these measurements on semiconductors and insulators.

In this paper, we present a direct method to determine the temperature at the apex of a semiconducting tip under laser illumination using L-APT. The method is based on the physics of the field evaporation process, i.e. on the known exponential dependence of the evaporation flux on the apex temperature. We apply this method to Si samples with different doping levels and show that the temperature reached under a green laser varies linearly with laser power and without significant dependence upon doping or tip shape.

2. Theoretical considerations

When exposed to a very high electric field F (~V/nm), an atom located at a surface has a finite probability to transition from its atomic to its ionic states and subsequently leave the surface. This phenomenon is called field evaporation and is induced by the lowering of the potential barrier Q for ionization as a result of the applied electric field [9]. Quantitatively, the probability φ for atom evaporation can be written in the form of an Arrhenius equation [9] i.e.

$$\varphi \propto \exp\left(-\frac{Q}{K_B T}\right) \qquad (1),$$

where K_B is the Boltzmann constant and T is the temperature of the surface. Based on eq. (1), it is clear that, if Q and φ were known, T could be calculated. The latter

is non-trivial as absolute values for φ or Q are not directly accessible. The problem becomes more tractable by realizing that eq. (1) also indicates that any reduction in barrier height (or increase in temperature) will lead to a corresponding exponential increase in evaporation probability. Hence rather than determining the absolute values for φ and Q, it will be sufficient to probe the change in φ with a change in barrier height Q in order to estimate the temperature at the moment of evaporation i.e.

$$T = \frac{-1}{K_B \left. \frac{d \ln \varphi}{dQ} \right|_T} \qquad (2).$$

To implement such a measurement, one thus has to vary the barrier height for evaporation and measure the resulting change in evaporation probability.

3. Experimental method

The difficulty in implementing the methodology suggested in eq. (2) lies in the fact that neither of the two quantities Q or φ are experimentally directly controllable. Firstly, the evaporation probability φ, is in principle a property to be determined for each individual evaporated atom. As is usually assumed [13,14], φ will therefore be estimated by considering that the measured evaporation flux, Φ (number of ions detected/pulse), is the integrated value of φ summed over the N^{apex} atoms of the emitting apex and averaged over a large number of pulses N_p. To ensure the required linear relation between the flux Φ and the evaporation probability φ, three experimental considerations had to be adopted. Firstly, all measurements were done at constant apex shape, i.e. φ averaged over the variations in evaporation probabilities at the atomic level across the tip apex is uniform. This ensures that the measured flux (atoms/pulse) is indeed a linear representation of φ. Secondly, measurements were done on low shank angle samples to negate the impact of a change in field of view, i.e. a change in the area of the emitting surface, on the measured flux. Thirdly, a sufficient number of atoms were collected for each measurement to minimize the impact of statistical noise via e.g. the difference in evaporation probabilities at the atomic level. It must also be noted that φ changes with time as the tip cools down. However, since atom probe measurements are carried at extremely low evaporation flux (0.01 – 0.08 atoms/pulse), φ quickly becomes orders of magnitude lower as soon as the tip starts to cool. Hence, the measured flux is a good representation of the evaporation probability at peak temperature. Under these assumptions, eq. (2) can readily be written as

$$T = \frac{-1}{K_B \left. \frac{d \ln \Phi}{dQ} \right|_T} \quad (3),$$

In order to calculate the change in barrier height Q we estimated the dependence of Q on V quantitatively using the relation proposed by Kreuzer and Nath [15], i.e.

$$Q = \left[\underbrace{\sqrt{1 - V/V_0} + \frac{1}{2}(V/V_0) \ln \left(\frac{1 - \sqrt{(1 - (V/V_0))}}{1 + \sqrt{(1 - (V/V_0))}} \right)}_{f(V/V_0)} \right] \times Q_0 \qquad (4),$$

where Q_0 is the barrier height at zero field, V_0 is the voltage required for evaporation at 0 K, V the applied DC voltage and V/V_0 is known as the voltage fraction. Eq. (4) shows that to determine the variations in Q with V, Q_0 and V/V_0 need to be determined but not V_0. Concerning Q_0, we use a value of $Q_0 = 5.86$ eV, which as obtained from first-principle molecular dynamic calculations [15]. Note, however, that values between 5.03 and 6.2 eV have also been reported in the literature [15–17]. The propagated error due to a possibly inaccurate value of Q_0 on the derived temperature value is discussed in the supplementary material but is less than 10%. Concerning V/V_0, it can be obtained experimentally in two different manners. First, as shown in **Fig. 1(A)** V_0 can be determined as the extrapolated voltage value at zero laser power of the voltage vs laser power curve (measured at constant flux) [18]. The results shown in Fig.1 (A) were obtained for four different Si tips and indicate that the resulting V_0 value is strongly tip (geometry)-dependent i.e. for every tip a different V_0 is obtained, ranging from 10 to 14 kV in the case of the tips of **Fig. 1(A)**). Such a variation would imply the necessity to pre-determine V_0 for every sample, making this approach very inconvenient. A second approach is to use the charge state fraction (CSF) defined as the relative Si^{2+} content, i.e. $Si^{2+}/(Si^{2+} + Si^{1+})$ which is known to correlate to the apex electric field, F [19] and by extension to F/F_0 (F_0 is the field required for evaporation at 0 K and is constant for a given material). The CSF vs F/F_0 curves are of course geometry independent and hence the CSF becomes a direct probe for F/F_0. As a consequence of the assumed proportionality between the field F at the apex and the applied voltage V [18], the CSF curves also provide then the V/V_0 values since $V/V_0 = F/F_0$. As shown in **Fig. 1(B)** where we determined the variations in CSF as a function of V/V_0 for the four Si tips already used in **Fig. 1(A)**, this approach is more attractive as the data are geometry-independent and overlap nicely. Hence the calibration curve needs to be established

only once which becomes much more convenient. Therefore, in this paper, we will only use this method and control the variations in Q quantitatively by looking at the CSF curves when varying the voltage to modify Q.

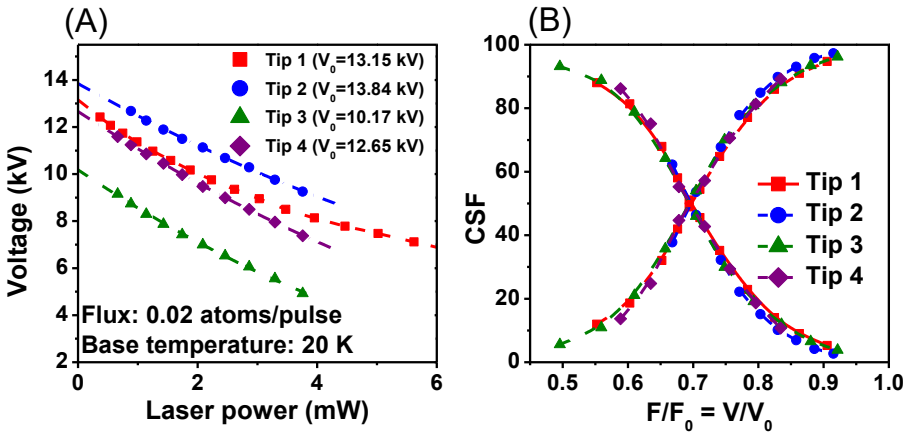

Figure 1. Illustration of the two methods proposed for the experimental determination of V/V_0 for four different Si tips. (A) Method 1: V_0 is extracted as the voltage required for field evaporation at zero laser power and is determined by extrapolation of the voltage vs laser power curve measured at constant flux (B) Method 2: V/V_0 is extracted from the measured CSF vs V/Vo curves, which are independent of the tip geometry as indicated by the overlapping data for all tips

Using eq. (3) and the above considerations to determine Q, the proposed experimental technique to derive the temperature at the tip apex is illustrated in **Fig. 2** for a Si tip illuminated by a green laser (wavelength =515 nm) at a power of 1.22 mW. First, as shown in **Fig. 2(A)**, the evaporation flux, at a constant laser power is recorded at different applied voltages (top x axis). At each applied voltage, the CSF is measured (bottom x axis), then translated, first, into V/V_0 using **Fig. 1(B)** and finally into Q using eq. (4). The correlation ln(Φ) vs Q, shown in **Fig. 2(B),** represents the expected linear relationship. Finally, the temperature at the apex is derived from the slope of this curve [20] based on the differential relation in eq. (3). In this example, the apex of the Si tip has reached a temperature of 427±15K. This value is consistent with other approaches discussed in literature to determine the temperature [4]. The estimated error on the temperature values is around $(\Delta T / T)$ ~ 10 % and arises from the random error when collecting 30 000 atoms for each measurement. For more information about the error propagation, we refer to the appendix.

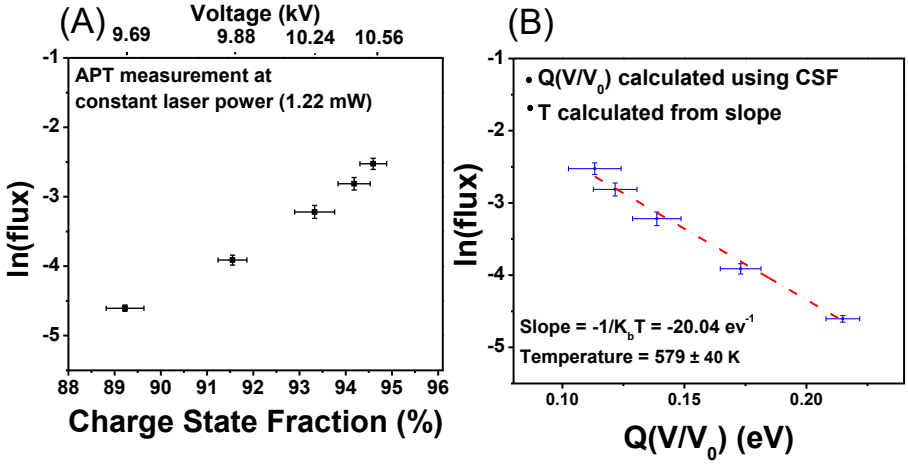

Figure 2. Summary of the proposed temperature measurement technique. (A) L-APT analysis is performed at constant laser power and the evaporation flux (left) is measured as a function of applied voltage. At the same time the different voltages are translated into CSF (bottom x axis). (B) After translating CSF into V/V_0 using fig. 1(B) and then into Q using eq. (3), the flux is plotted as a function of Q. The slope of the linear regression for the ln(flux) vs. Q relationship, then leads to the temperature value based on eq. (2).

4. Sample preparation and measurement procedure

Tips suitable for L-APT measurements were prepared by the lift out method and sub-sequential annular focused ion beam (FIB) milling [21], using a FEI NOVA-600 dual beam tool. To limit the amorphization of the surface by the ion beam an in-situ Pt cap was deposited prior to lamella preparation. The APT analysis was done with the Laser Assisted Wide Angle Tomographic Atom Probe (LAWATAP) from Cameca using laser pulsing (wavelength 515 nm, 400 fs pulse duration, 10 kHz repetition rate) at 80 K sample temperature. L-APT measurements were done on Si samples. To calculate the temperature the applied voltage was varied to maintain the pre-defined flux at constant laser power. Each measurement consisted 5-6 flux conditions and 30 000 atoms were collected at each flux. To check the impact of number of atoms collected per measurement limited measurements were also done using 0.8×10^5 - 1×10^6 atoms per flux however, negligible impact was observed on the temperature measure. Collecting more atoms per measurement decreased the random error/noise in the CSF (see Appendix) however, lower atom counts were chosen in the lieu of reduced time of the measurement.

When starting a fresh sample or when changing the laser power between experiments, 1 – 2 million atoms were collected to make sure the tip had reached its equilibrium shape. To judge the impact of apex shape, experiment sets consisting of various laser powers were repeated on the same and fresh samples. The experiments resulted in the same calculated temperature value (within the error bar) for a given laser power (Figure 4). The high repeatability of the measurements illustrates a negligible impact of the apex shape of the tip on measured temperature values and points to inexistence to transient shapes during the measurement at a constant laser power.

Field evaporation of Si clusters and its subsequent dissociation was initially a concern at higher laser powers as it might have impacted the measured CSF. However, as can be seen from the mass spectra in **Fig. 3**, no Si clusters were observed at higher laser powers.

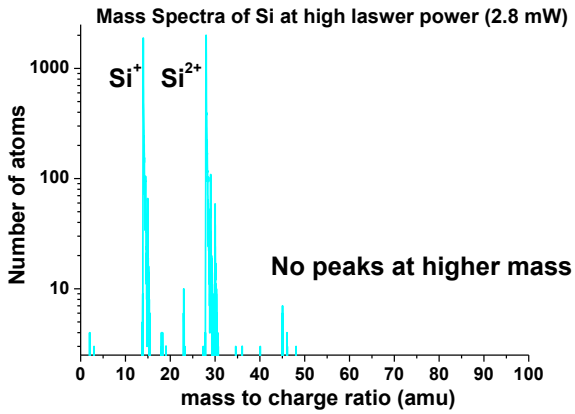

Figure 3. Mass spectra Si at high laser power (2.8mW). No Si clusters were observed in the spectra.

5. Application and discussion of the results

Having established the methodology to determine the apex temperature, it is now interesting to address the insight which can be generated in various processes linked to the laser-tip interaction. As a first case study, we investigated the dependence of the temperature at the apex on laser power, impurity type and doping level

Temperature measurements were done on four Si samples with substantially different doping levels whereby two were n-type doped ($4x10^{14}$ atoms/cm^3 and $5x10^{19}$ atoms/cm^3) and the other two were p-type doped ($3x10^{15}$ atoms/cm^3 and 10^{19}

atoms/cm^3). For each sample, a series of measurements was done covering a laser power range between 0.7 mW to 3 mW. As shown in **Fig. 4a**, in each case the linear relation for ln(Φ) vs Q, was found confirming the consistency of our approach.

The temperature values derived from the slope of these curves, **Fig. 4b**, range from ~300 K to ~1250 K for laser powers between 0.7 mW and 3 mW. A linear dependence of the temperature on laser power is observed over a temperature range from 300 K up to ~ 1250 K (which is close to the melting point of Si). These results imply that over the laser power range investigated, non-linear absorption effects (multiphoton absorption) are *not* observed. Within the error bar, the temperatures induced by the laser pulse are independent of the doping level and dopant type for the different tips. This points towards a negligible effect of free-carrier absorption, which was to be expected given the relatively moderate optical power range [22].

For the (low) laser powers used under normal L-APT conditions i.e. the laser provides only ~10-20% of the energy for field evaporation, we obtain moderate temperatures (300 K-550 K) comparable to the values reported in literature for metals [4,8]. At high laser power, temperatures close to the melting point of Si are reached (~1250 K). Consistent with these values is the fact that Si tips under slightly higher power illumination start to show signs of local melting [23]. Moreover, since in this case the laser provides nearly 60% of the energy for field evaporation, the evaporation becomes essentially thermal.

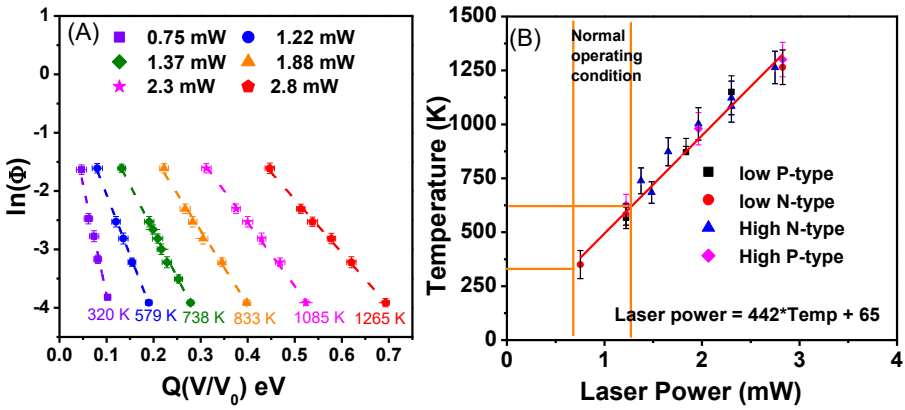

Figure 4. (a) Experimental ln(Φ) vs Q(V/V_0) and (b) extracted temperature as a function of laser power on tips with different n- and p-type doping levels. For normal operating conditions (10-20% of the energy provided by the laser for field evaporation) a temperature between 300 K and 550 K is obtained.

6. Conclusion

This work presents a method to determine the temperature of a nanoscale tip under laser pulsing at the moment of atom evaporation in L-APT. The method is based on measuring the variation in evaporation flux as a function of the applied voltage at fixed laser power and can provide temperatures with a relative error below 10 %. The strength of this approach is that it samples the temperature at the exact moment of the atom evaporation.

We showed that the temperature at the apex of a Si tip illuminated with a green pulsed laser varies linearly between ~300 K and ~1250 K using laser powers between 1 and 3 mW. Of course, applicability to other wavelengths and material systems is straightforward. The method has provided useful insight into laser-assisted field evaporation in biased nanoscale Si specimens. To begin with, no major impact of nonlinear optical or thermal phenomena in Si samples has been noticed. Similarly, no impact of doping is to be reported. Similarly, by performing the analysis using atoms evaporated from particular regions on the tip surface, this work can be extended towards studying the temperature distribution across the tip apex.

References

[1] I.S. Averbukh, B.M. Chernobrod, O.A. Sedletsky, Y. Prior, Coherent near field optical microscopy, Opt. Commun. 174 (2000) 33–41. doi:10.1016/S0030-4018(99)00696-3.

[2] A.V. Zayats, T. Kalkbrenner, V. Sandoghdar, J. Mlynek, Second-harmonic generation from individual surface defects under local excitation, Phys. Rev. B. 61 (2000) 4545–4548. doi:10.1103/PhysRevB.61.4545.

[3] Y. Kawata, C. Xu, W. Denk, Feasibility of molecular-resolution fluorescence near-field microscopy using multi-photon absorption and field enhancement near a sharp tip, J. Appl. Phys. 85 (1999) 1294–1301. doi:10.1063/1.369260.

[4] A. Vella, On the interaction of an ultra-fast laser with a nanometric tip by laser assisted atom probe tomography: a review, Ultramicroscopy. 132 (2013) 5–18. doi:10.1016/j.ultramic.2013.05.016.

[5] J. Bunton, J. Olson, D. Lenz, T. Kelly, Investigation of Performance-Influencing Factors in Pulsed Laser Atom Probe, Microsc. Microanal. 14 (2008) 1238–1239. doi:10.1017/S143192760808642X.

[6] A. Kumar, M.P. Komalan, H. Lenka, A.K. Kambham, M. Gilbert, F. Gencarelli, B. Vincent, W. Vandervorst, Atomic insight into Ge1−xSnx using atom probe tomography, Ultramicroscopy. 132 (2013) 171–178. doi:10.1016/j.ultramic.2013.02.009.

[7] J.R. Riley, R.A. Bernal, Q. Li, H.D. Espinosa, G.T. Wang, L.J. Lauhon, Atom Probe Tomography of a-Axis GaN Nanowires: Analysis of Nonstoichiometric Evaporation Behavior, ACS Nano. 6 (2012) 3898–3906. doi:10.1021/nn2050517.

[8] A. Cerezo, G.D.W. Smith, P.H. Clifton, Measurement of temperature rises in the femtosecond laser pulsed three-dimensional atom probe, Appl. Phys. Lett. 88 (2006) 154103. doi:10.1063/1.2191412.

[9] T.T. Tsong, Atom-Probe Field Ion Microscopy: Field Ion Emission, and Surfaces and Interfaces at Atomic Resolution, Cambridge University Press, 2005.

[10] G.L. Kellogg, Determining the field emitter temperature during laser irradiation in the pulsed laser atom probe, J. Appl. Phys. 52 (1981) 5320–5328. doi:10.1063/1.329390.

[11] E.A. Marquis, B. Gault, Determination of the tip temperature in laser assisted atom-probe tomography using charge state distributions, J. Appl. Phys. 104 (2008) 084914. doi:10.1063/1.3006017.

[12] B. Gault, F. Vurpillot, A. Vella, M. Gilbert, A. Menand, D. Blavette, B. Deconihout, Design of a femtosecond laser assisted tomographic atom probe, Rev. Sci. Instrum. 77 (2006) 043705. doi:10.1063/1.2194089.
[13] F. De Geuser, B. Gault, A. Bostel, F. Vurpillot, Correlated field evaporation as seen by atom probe tomography, Surf. Sci. 601 (2007) 536–543. doi:10.1016/j.susc.2006.10.019.
[14] M. Gruber, F. Vurpillot, A. Bostel, B. Deconihout, Field evaporation: A kinetic Monte Carlo approach on the influence of temperature, Surf. Sci. 605 (2011) 2025–2031. doi:10.1016/j.susc.2011.07.022.
[15] T. Ono, K. Hirose, First-principles study on field evaporation for silicon atom on Si(001) surface, J. Appl. Phys. 95 (2004) 1568–1571. doi:10.1063/1.1636258.
[16] N.M. Miskovsky, C.M. Wei, T.T. Tsong, Field evaporation of silicon in the field ion microscope and scanning tunneling microscope configurations, Phys. Rev. Lett. 69 (1992) 2427–2430. doi:10.1103/PhysRevLett.69.2427.
[17] I.-W. Lyo, P. Avouris, Field-Induced Nanometer- to Atomic-Scale Manipulation of Silicon Surfaces with the STM, Science. 253 (1991) 173–176. doi:10.1126/science.253.5016.173.
[18] B. Mazumder, A. Vella, M. Gilbert, B. Deconihout, G. Schmitz, Reneutralization time of surface silicon ions on a field emitter, New J. Phys. 12 (2010) 113029. doi:10.1088/1367-2630/12/11/113029.
[19] D.R. Kingham, The post-ionization of field evaporated ions: A theoretical explanation of multiple charge states, Surf. Sci. 116 (1982) 273–301. doi:10.1016/0039-6028(82)90434-4.
[20] D. York, N.M. Evensen, M.L. Martínez, J.D.B. Delgado, Unified equations for the slope, intercept, and standard errors of the best straight line, Am. J. Phys. 72 (2004) 367–375. doi:10.1119/1.1632486.
[21] J.H. Bunton, J.D. Olson, D.R. Lenz, T.F. Kelly, Advances in Pulsed-Laser Atom Probe: Instrument and Specimen Design for Optimum Performance, Microsc. Microanal. 13 (2007) 418–427. doi:10.1017/S1431927607070869.
[22] E.P. Silaeva, A. Vella, N. Sevelin-Radiguet, G. Martel, B. Deconihout, T.E. Itina, Ultrafast laser-triggered field ion emission from semiconductor tips, New J. Phys. 14 (2012) 113026. doi:10.1088/1367-2630/14/11/113026.

[23] J. Bogdanowicz, M. Gilbert, S. Koelling, W. Vandervorst, Impact of the apex of an elongated dielectric tip upon its light absorption properties, Appl. Surf. Sci. 302 (2014) 223–225. doi:10.1016/j.apsusc.2013.10.150.
[24] E.W. Müller, Field Desorption, Phys. Rev. 102 (1956) 618–624. doi:10.1103/PhysRev.102.618.
[25] R. Gomer, Field emission, field ionization, and field desorption, Surf. Sci. 299–300 (1994) 129–152. doi:10.1016/0039-6028(94)90651-3.
[26] R.G. Forbes, Field evaporation theory: a review of basic ideas, Appl. Surf. Sci. 87–88 (1995) 1–11. doi:10.1016/0169-4332(94)00526-5.

Appendix

Error Analysis

The accompanying paper describes a method for deriving experimentally the temperature at the apex of a sharp nanoscale tip. In summary, the temperature is obtained based on the evaluation of the variation in laser-assisted field-evaporation flux Φ when varying the barrier height Q for evaporation, i.e.

$$T = -\frac{1}{K_B} \times \frac{dQ}{d\ln(\Phi)} \qquad (1).$$

Any error ΔQ on the barrier height or $\Delta\Phi$ on the evaporation flux will propagate into an error ΔT on the temperature. Two types of errors, i.e. *systematic* and *random*, must be distinguished. On the one hand, the systematic error is the error induced by potentially erroneous modelling, i.e. it is independent from the measurement statistics. The magnitude of this error, i.e. the accuracy of the technique, is discussed in Section 1.1. On the other hand, the random error results from the statistical variations on the experimentally measured parameters, i.e. Φ and CSF. The magnitude of this error, i.e. the precision of the technique, is discussed in Section 1.2.

1.1 Systematic error

A systematic error on the derived temperature can stem from potentially erroneous modeling of $Q(V/V_0)$ or V_0. We here evaluate how to minimize this systematic error and how these potential errors propagate into an error on the measured temperature.

Systematic error due to inaccurate $Q(V/V_0)$

Let us start with recommendations on the use of the different $Q(V/V_0)$ models available in the literature, i.e. respectively the Mueller – Schottky model and Gomer's charge-exchange model [1,2], and evaluate the magnitude of the systematic error we can expect on the temperature values derived in this paper. In this paper, we only used the charge-exchange model as it proved to be more accurate [3]. To show this experimentally, we looked at the

experimental behavior of the locus of constant flux in the (V/V_0, P) space, where P is the incident laser power (**Fig 1**). Theoretically, Arrhenius law predicts that the locus of constant flux in the (Q, T) plane should be a straight line. This is also true for the locus of constant flux in the (Q, P) plane assuming the apex temperature depends linearly on laser power (see e.g. Fig. 3(B) of the accompanying paper). As a result, in the experimental (V/V_0, P) plane of Fig. 1, the nonlinearity of the locus of constant flux is characteristic of the $Q(V/V_0)$ dependence. In other words, a valid theoretical model of the $Q(V/V_0)$ dependence should be able to predict accurately the experimental shape of the locus of constant flux in the (V/V_0, P) plane. Yet, as Fig. 1 shows, only the charge-exchange model can fit the shape of the experimental locus of constant flux in the (V/V_0, P) plane (**Fig. 1**) and it is therefore recommended that only the latter model should be used.

Nonetheless, when using the charge-exchange model, the barrier height depends on the parameter Q_0, i.e. the barrier height at zero fields (eq. 6 of accompanying paper). If an error is made on Q_0, it will therefore propagate such that $\Delta T / T = \Delta Q_0 / Q_0$. For Si, Q_0 values ranging between 5.03 – 6.2 eV have been reported in literature [4–6] such that no more than ~8% error should be expected on the temperature values mentioned in this paper. Let us also importantly note that since Q_0 is only a multiplicative term in Q (eq. 6 of companion paper), the relative temperature variations will still be accurate and independent of Q_0. Hence, the presented method remains an excellent error-free tool for comparative studies as long as the material and hence Q_0 remain the same.

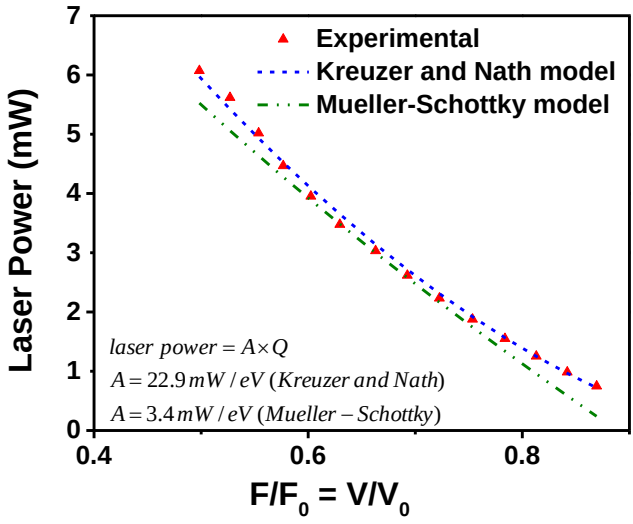

Figure A1: Experimental verification of the charge exchange and the Mueller-Schottky model. The fitting parameter is the proportionality constant between P and Q(V/V_0) and is equal to 22.9 mW/eV and 3.4 mW/eV for the charge exchange and image hump model respectively. Please note, the mathematical treatment used for the charge exchange model is the one developed by Kreuzer and Nath [4]. As can be seen the charge exchange model can correctly predict the change in barrier height with applied field for a larger range of field as compared to the Mueller – Schottky model.

Systematic error due to inaccurate V_0 value

Another potential source of systematic error is the value of V_0, i.e. the threshold voltage for field evaporation at a 0 K temperature. In this paper, V_0 was obtained as the ordinate (at P = 0) of the constant-flux locus in the (V, P) space, assuming a linear dependence of the temperature as a function of laser power (Fig. 1(A) of companion paper). In other words, the obtained value is actually the value of the threshold voltage for field evaporation at a 15 K temperature, since the holder and hence the tip are kept at that base temperature during the measurement. This leads to an underestimated V_0 value. In order to quantify the resulting underestimation, we compared the V_0

values obtained respectively at 15 K and 80 K base temperatures. Since we obtained a difference of about 1 kV, we speculate that, by extrapolation, the underestimation of V_0 is no more than ~0.23 kV when using the value obtained at a 15 K base temperature.

Let us now prove that this underestimation has only a very marginal impact on the derived temperature. For this purpose, we have deliberately varied the value of V_0 and evaluated the resulting variation in obtained temperature on the set of experimental data used in Fig. 2 of the companion paper (V_0 = 13 kV at a 15 K base temperature for tip 1 in accompanying paper). As can be observed in Fig. 2(A), the value of V_0 hardly impacts the slope of the (V/V_0, Q) characteristic in spite of the large variations in V_0. As a result, Fig. 2(B) shows that the measured temperature is virtually independent from the V_0 value for $V_0 \leq 17$ kV, i.e. even a 4 kV error would be acceptable. In conclusion, though the error on V_0 should be kept under control, a small error does not propagate significantly on the temperature value. This conclusion is a direct consequence of a combination of two inherent advantages of the developed method. Firstly, in the range of CSF used to calculate temperature, Q can be approximated to vary linearly with V/V_0 (fig. 2(A)). Secondly, because the temperature is obtained using a differential (eq. 1), it is

independent of V_0 provided the probed Q range is small enough to ensure the linearity of the relationship between Q and V/V_0.

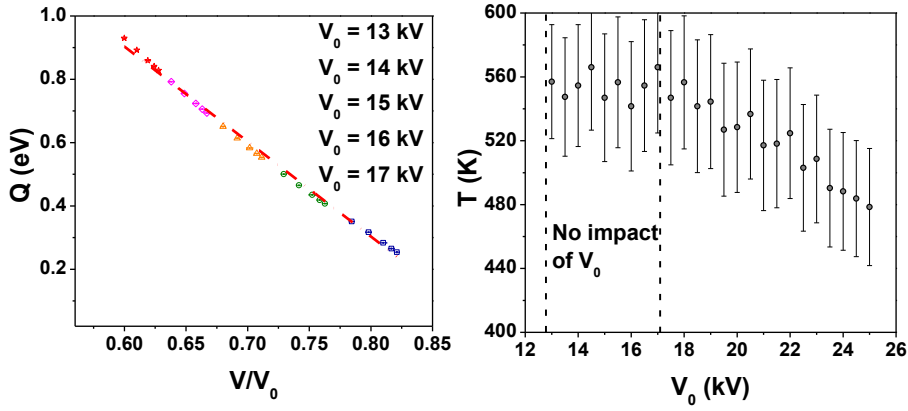

Figure A2: (A) Barrier height as a function of V/V_0. Each data set is calculated by deliberately overestimating the V_0 and thereafter calculating the Q using the same set of experimental CSF values. As can be seen, over a range of V_0 values (V_0 = 13 – 17 kV), $\partial Q/\partial(V/V_0)$ is independent of V_0. Hence the temperature values, calculated using V_0 = 13 – 17 kV and the same set of experimental Φ and CSF, are similar (Fig. 2(B)). However, for V_0 > 17 kV Q cannot be approximated to vary linearly with V/V_0, i.e. $\partial Q/\partial(V/V_0)$ is dependent of V_0. Hence, the derived temperature values vary with V_0 (Fig. 2(B)).

1.2. Random Error

The random error on T originates from the statistical noise on the two experimental parameters, Φ and CSF. Obviously, increasing the number of measured atoms N reduces this random error but for the sake of measurement time, N was restricted to approximately $3x10^4$ atoms in this paper. Let us first estimate the relative errors $\Delta Q/Q$ and $\Delta\ln(\Phi)/\ln(\Phi)$ and then estimate how they will impact the measured temperature value.

Looking first at the random error on the evaporation flux, let us remind that the flux can be modeled as a Poisson process [7]. As a result, the random error on the flux can readily be obtained as the counting statistic error on a Poisson distribution, i.e. $\Phi\sqrt{\Phi/N}$, where N is the number of atoms per data point. The relative error on Φ is therefore ~ ±0.08% for $N=3x10^4$ atoms as we used in this paper. In other words, the random error on the flux is extremely low and can be expected to have only a very marginal impact on the T value.

Concerning the random error on the CSF, it was calculated by first dividing the collected set of N atoms into smaller blocks of atoms (2500 atoms/block, i.e. 12 blocks). The random error on CSF was then calculated as the standard deviation of the distribution of the average CSF in each individual block. For N=3x10^4 atoms, we obtained $\Delta CSF/CSF \sim \pm 1\%$ for a block size of 2500 atoms. In other words, ΔCSF clearly dominates ΔΦ. As we show below, it also has a much higher impact on the T value.

Let us now evaluate the error on the temperature value induced by the random error on CSF and ln(Φ) by means of a Monte Carlo approach (Fig. 3). Using the experimental data of Fig. 2 of the accompanying paper, we quantified the relative error ΔT/T as a function of ΔCSF/CSF and Δln(Φ)/ln(Φ) by letting CSF and ln(Φ) randomly vary between $|1-\Delta x/x|x$ and $|1+\Delta x/x|x$ (x=CSF or ln(Φ)) before calculating the resulting temperature. For each value of ΔCSF/CSF and Δln(Φ)/ln(Φ), this random process was repeated 10^4 times to generate a temperature probability distribution. ΔT/T was then calculated from the resulting probability distribution as $\Delta T/T = 2\sigma/\mu$, where σ is the standard deviation and μ is the mean of the distribution. As shown in Figure 3, in this paper, $\Delta T/T \sim 10\%$ for the above mentioned Δln(Φ)/ln(Φ) ~0.04% and $\Delta CSF/CSF \sim 1\%$. Figure 3 also shows that ΔCSF/CSF has a higher impact as compared Δln(Φ)/ln(Φ). This is so because the range of CSF ($CSF_{max} - CSF_{min} \sim 6\%$) probed to calculate temperature leads to a Q variation of the order of ($Q_{max} - Q_{min} \sim 0.1$ eV) which is much smaller than the corresponding change in ln(Φ ($\ln(\Phi)_{max} - \ln(\Phi)_{min} \sim 2.5$). Hence, an error on Q will allow for a greater swing in the slope and hence a higher uncertainty. In other words, to minimize the random error on T, we not only recommend a large counting statistic but also a wide range of CSF. Note that, on the other hand, care should be taken that Q values (resulting from the CSF) can still be approximated to vary linearly with V/V_0 so as to minimize the systematic error due to the underestimated V_0 (see above). Furthermore, the multi hits and DC evaporation resulting at high fluxes should also be kept under control. For Si it was observed that a change of CSF, i.e. $CSF_{max} - CSF_{min} \sim 6 - 8\%$ was optimum for low random and systematic errors.

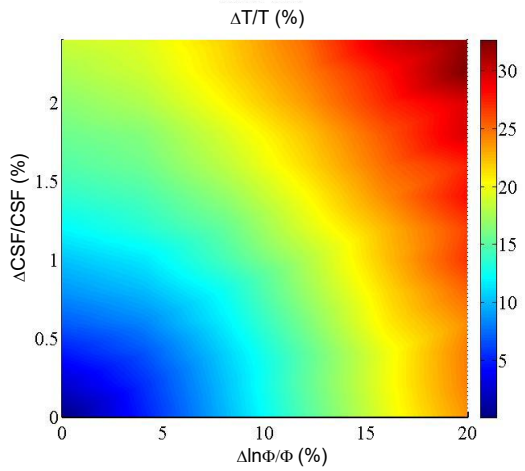

Figure A3: Monte-Carlo plot for the random error on the derived temperature values due to a random error on ln(Φ) and CSF. The experimental data shown in fig. 2 of accompanying paper was used to calculate this plot.

To conclude, Q_0 is the main source of systematic error on the derived temperature value, leading in Si to a potential 8% error. As we noted, however, the technique can derive T/Q_0 without accuracy loss. Regarding random errors, they originate from the statistical noise on the experimental parameters CSF and Φ. Using counting statistics of $N=5\times10^4$ atoms, an 8% random error on T is expected, mostly propagating from the random error on the CSF.

References

[1] E.W. Müller, Field Desorption, Phys. Rev. 102 (1956) 618–624. doi:10.1103/PhysRev.102.618.

[2] R. Gomer, Field emission, field ionization, and field desorption, Surf. Sci. 299–300 (1994) 129–152. doi:10.1016/0039-6028(94)90651-3.

[3] R.G. Forbes, Field evaporation theory: a review of basic ideas, Appl. Surf. Sci. 87–88 (1995) 1–11. doi:10.1016/0169-4332(94)00526-5.

[4] I.-W. Lyo, P. Avouris, Field-Induced Nanometer- to Atomic-Scale Manipulation of Silicon Surfaces with the STM, Science. 253 (1991) 173–176. doi:10.1126/science.253.5016.173.

[5] N.M. Miskovsky, C.M. Wei, T.T. Tsong, Field evaporation of silicon in the field ion microscope and scanning tunneling microscope configurations, Phys. Rev. Lett. 69 (1992) 2427–2430. doi:10.1103/PhysRevLett.69.2427.

[6] T. Ono, K. Hirose, First-principles study on field evaporation for silicon atom on Si(001) surface, J. Appl. Phys. 95 (2004) 1568–1571. doi:10.1063/1.1636258.